KSME

Springer

Journal of Mechanical Science and Technology 34 (2) 2020

Original Article
DOI 10.1007/s12206-020-0129-0

Keywords:
· Angular contact ball bearing
· Contact angles
· The triangular geometric theorem
· Vector diagram method

Correspondence to:
Jin-hua Zhang
jjshua@mail.xjtu.edu.cn

Citation:
Zhang, J., Fang, B., Yan, K., Hong, J. (2020). A novel model for high-speed angular contact ball bearing by considering variable contact angles. Journal of Mechanical Science and Technology 34 (2) (2020) 809~816.
http://doi.org/10.1007/s12206-020-0129-0

Received October 7th, 2018
Revised October 7th, 2019
Accepted December 17th, 2019

† Recommended by Editor Hyung Wook Park

A novel model for high-speed angular contact ball bearing by considering variable contact angles

Jin-hua Zhang[1,2], Bin Fang[1,2], Ke Yan[1] and Jun Hong[1,2]

[1]Key Laboratory of Education Ministry for Modern Design and Rotor-Bearing System, Xi'an Jiaotong University, Xi'an 710049, China, [2]School of Mechanical Engineering, Xi'an Jiaotong University, Xi'an 710049, China

Abstract In this study, on the basis of the various contact angles and the hybrid theory, a new mathematic model without the raceway control hypothesis is proposed for the analysis of ball bearing under the combined axial, radial and moment loads. Instead of the orthogonal decomposition method, the triangular geometric theorem and vector diagram method have been used in the force analysis of local ball to improve the computation efficiency of bearing analysis. For validation purpose, the comparative analysis of the ball-raceway contact angles and loads of ball bearing under different operation conditions obtained by the proposed model and the Jones' model with different raceway control hypotheses has been conducted. The results show that the proposed model has a higher applicability and rationality compared to the Jones' model, and a proper moment load can be used to improve the load distribution and service performance of ball bearing subjected to the radial load.

1. Introduction

Ball bearings as the core supporting and motion transmission components, are widely used in numerous rotating machinery. The dynamic behaviors of ball bearings have a significant effect on the service performance of the rotor-bearing system.

In order to accurately predict the dynamic behaviors of ball bearing, a large number of studies on ball bearing modeling have been presented in the past decades. In the earlier researches conducted by Stribeck [1], Sjovall [2], Lundberg and Palmgren [3, 4], the load distribution, deformation and various service parameters of ball bearing under different load conditions are determined by some empirical formulations. However, due to the ignorance of the inertia forces of balls, these models cannot be used in the accurate calculation of ball bearing at high speed range. Based on the raceway control hypothesis, Jones [5] firstly proposed a theoretical model for high-speed ball bearing under the combined axial, radial and moment loads, and the effect of ball centrifugal force and gyroscopic moment has been fully considered. As the most classical theoretical model of ball bearing, Jones' model provided important guidance for the presentation and improvement of the subsequent models. Based on the results of ball bearing under different operation conditions calculated by the Jones' model, Harris [6] found that the raceway control hypothesis has many limitations and is only suitable for a few working conditions of ball bearing. To overcome the defects of the raceway control hypothesis, several improved models of ball bearing without raceway control hypothesis have been proposed in recent years [7-9]. In addition, Harris [10] proposed a new analytical model based on the lubrication analysis of ball-raceway contacts to investigate the skidding behaviors of the axially loaded ball bearing at high speed range. Above all, an effective and accurate mathematic model is the foundation for the preformation prediction and analysis of ball bearing.

Based on the summary of literatures for ball bearing modeling, it can be found that the dynamic parameters of ball bearing including the ball-raceway contact angles and contact loads et al. can be obtained by solving the nonlinear equations, and the nonlinear equations in ball bearing modeling can be divided into two categories: The local equilibrium equations of balls and the global equilibrium equations of ring. For example, in the Jones' model, 4*Z local variables of balls (Z denotes the number of balls) and 3 or 5 global variables of ring have been used in the bearing modeling. It means that the number of nonlinear equations increases rapidly with the increase of ball number Z, and it also causes a sharply increase in the computation load and time consuming for ball bearing analysis. In order to improve the computational efficiency of ball bearing, Liao and Lin [11-13] developed a new method for analyzing the deformations and loads of ball bearing with variable contact angles. However, this model not only neglected the effect of the gyroscopic moment of ball, but also adopt the assumption that the osculation of the inner and outer raceways are the same, it may cause a large error for ball bearing under some specific conditions [14]. Based on the Jones model and outer raceway control hypothesis, Antoine [15] presented a new method for the explicit contact angle calculation for ball bearing under the pure axial load, and then the model has been further extended to deal with ball bearing under the combined loads [16]. Above all, the above simplified models were mostly based on some certain assumptions. Although the calculation of the bearing model can be reduced to some extent, the calculation error of the bearing analysis is more or less increased. In addition, compared to the Jones' model, the use of variable contact angles in the local analysis of balls is more conducive to the selection of the initial value in the iterative calculation of ball bearing.

In this paper, in order to improve the calculation accuracy and efficiency of ball bearing analysis, a novel model for high-speed ball bearing under the combined axial, radial and moment loads is presented based on the various contact angles and the hybrid theory without raceway control hypothesis. Instead of the orthogonal decomposition method, the triangular geometric theorem and vector diagram method have been used in the local force analysis of ball to improve the computation efficiency of the proposed model. On this basis, the contact angles, contact loads and displacements of ball bearing under different working conditions are calculated and discussed. Besides, the results are compared with those from Jones' model with different raceway control hypotheses to verify the correctness of the proposed model.

2. Theoretical analysis

As shown in Fig. 1(a), in order to study the dynamic performance of ball bearing under the combined axial, radial and moment loads. It is assumed that the outer ring is fixed and and the inner ring rotates with the shaft, and the relative displacement vector of the inner ring with respect to outer ring of ball bearing is **d** = {$\delta_x, \delta_y, \delta_z, \theta_y, \theta_z$} under the action of the external load vector **F** = {F_x, F_y, F_z, M_y, M_z}. On this basis, for the ball at any position angular ψ_k, the geometry and mechanical relations among the ball and rings are presented in Fig. 1, with the increase of rotating speed, the center of ball moves upward from the point O_b to point O_b' under the action of centrifugal force, and the curvature center of inner raceway also shifts from the point O_i to point O_i' under the action of external loads. Therefore, the ball-inner raceway contact angle α_{ik} increases, while the ball-outer raceway contact angle α_{ok} decreases.

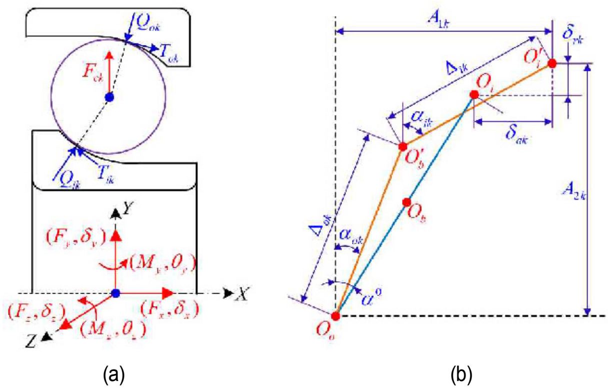

Fig. 1. The geometry and mechanical relations of ball and rings: (a) The mechanical state; (b) the geometry state.

As shown in Fig. 1(b), the final distances between the curvature centers of inner and outer raceways in the horizon and vertical directions can be expressed as:

$$\begin{cases} A_{1k} = (r_i + r_o - D)\sin\alpha^0 + \delta_{ak} \\ A_{2k} = (r_i + r_o - D)\cos\alpha^0 + \delta_{rk} \end{cases} \quad (1)$$

where r_i and r_o are the curvature radii of inner and outer raceways, D is the diameter of ball, and α^0 is the initial contact angle of ball bearing. In addition, δ_{ak} and δ_{rk} are the relative displacements of inner ring with respect to outer ring at any angular position ψ_k:

$$\begin{cases} \delta_{ak} = \delta_x + 0.5d_m \sin\psi_k\theta_y - 0.5d_m \cos\psi_k\theta_z \\ \delta_{rk} = \cos\psi_k\delta_y + \sin\psi_k\delta_z \end{cases} \quad (2)$$

where d_m denotes the pitch diameter of ball bearing.

As shown in Fig. 1(b), the final distances between the curvature centers of inner and outer raceways A_{1k} and A_{2k} can also be expressed by the final contact angles α_{ik}, α_{ok} and the final distances between the centers of ball and inner/outer raceway curvature Δ_{ik}, Δ_{ok}:

$$\begin{cases} \Delta_{ik}\sin\alpha_{ik} + \Delta_{ok}\sin\alpha_{ok} - A_{1k} = 0 \\ \Delta_{ik}\cos\alpha_{ik} + \Delta_{ok}\cos\alpha_{ok} - A_{2k} = 0 \end{cases} \quad (3)$$

where Δ_{ik} and Δ_{ok} can be written as:

$$\begin{cases} \Delta_{ik} = r_i - 0.5D + \delta_{ik} \\ \Delta_{ok} = r_o - 0.5D + \delta_{ok} \end{cases} \quad (4)$$

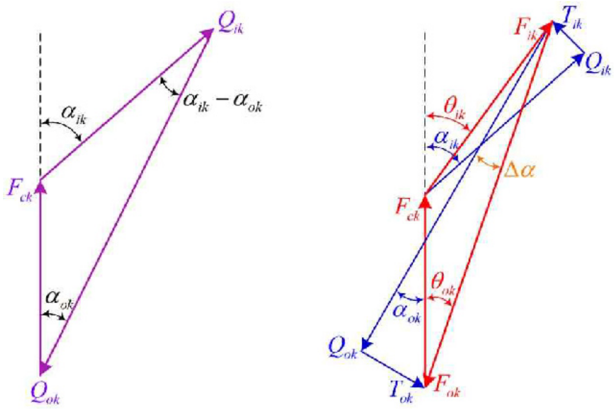

(a) (b)

Fig. 2. The force vector diagrams of ball: (a) Without the gyroscopic moment of ball; (b) with the gyroscopic moment of ball.

where δ_{ik} and δ_{ok} are the contact deformations of ball-inner raceway and ball-outer raceway, respectively. According to the Hertz theory of point contact, δ_{ik} and δ_{ok} can be expressed as:

$$\begin{cases}\delta_{ik}=\left(\dfrac{Q_{ik}}{K_{ik}}\right)^{2/3}\\ \delta_{ok}=\left(\dfrac{Q_{ok}}{K_{ok}}\right)^{2/3}\end{cases} \tag{5}$$

where Q_{ik} and Q_{ok} denote the contact loads of ball-inner raceway and ball-outer raceway, respectively, and the K_{ik} and K_{ok} are the load-deformation coefficients of ball-inner raceway and ball-outer raceway, respectively.

In order to obtain the explicit expressions of contact loads Q_{ik} and Q_{ok}, the vector diagram method is applied in the force analysis of ball instead of the orthogonal decomposition method. For comparison, the mechanical state of ball without considering the gyroscopic moment is given first. As shown in Fig. 2(a), the vector equilibrium equation of ball can be written as:

$$\overrightarrow{F_{ck}}+\overrightarrow{Q_{ik}}+\overrightarrow{Q_{ok}}=0 \tag{6}$$

where $\overrightarrow{F_{ck}}$ is the vector of ball centrifugal force, according to the sine theorem of plane triangle, one can obtain:

$$\frac{Q_{ik}}{\sin\alpha_{ok}}=\frac{Q_{ok}}{\sin\alpha_{ik}}=\frac{F_{ck}}{\sin\left(\alpha_{ik}-\alpha_{ok}\right)} \tag{7}$$

$$\begin{cases}Q_{ik}=\dfrac{\sin\alpha_{ok}}{\sin\left(\alpha_{ik}-\alpha_{ok}\right)}F_{ck}\\ Q_{ok}=\dfrac{\sin\alpha_{ik}}{\sin\left(\alpha_{ik}-\alpha_{ok}\right)}F_{ck}\end{cases} \tag{8}$$

When the gyroscopic moment of ball is taken into account, as shown in Fig. 2(b), the vector equilibrium equation of ball can be rewritten as:

$$\overrightarrow{F_{ck}}+\overrightarrow{Q_{ik}}+\overrightarrow{T_{ik}}+\overrightarrow{Q_{ok}}+\overrightarrow{T_{ok}}=0 \tag{9}$$

where $\overrightarrow{T_{ik}}$ and $\overrightarrow{T_{ok}}$ are the friction forces in ball-inner raceway and ball-outer raceway contacts, respectively. Since the friction forces are used to offset the action of ball gyroscopic moment, the follow expressions can be obtained:

$$\begin{cases}T_{ik}=\lambda_{ik}\dfrac{2M_{gk}}{D}\\ T_{ok}=\lambda_{ok}\dfrac{2M_{gk}}{D}\end{cases} \tag{10}$$

where M_{gk} is the gyroscopic moment of ball.

$$\lambda_{ik}+\lambda_{ok}=1 \tag{11}$$

In order to further determine the sizes of T_{ik} and T_{ok}, several different allocation schemes of the frictions were given in previous literatures, and the most representative allocation methods are given by Jones based on the Raceway Control Hypothesis:

Inner Raceway Control Hypothesis: $\lambda_{ik}=0.5$ and $\lambda_{ok}=0.5$;

Outer Raceway Control Hypothesis: $\lambda_{ik}=0$ and $\lambda_{ok}=1$.

However, the follow up studies showed that the above allocation schemes based on the raceway control hypothesis presented an obvious speed-discontinuity. To overcome this defect, an improve allocation scheme of the frictions in ball-raceway contacts was given based on the equal friction coefficient assumption [8].

$$\mu=\frac{T_{ik}}{Q_{ik}}=\frac{T_{ok}}{Q_{ok}}=\frac{1}{Q_{ik}+Q_{ok}}\frac{2M_{gk}}{D} \tag{12}$$

$$\begin{cases}T_{ik}=\dfrac{Q_{ik}}{Q_{ik}+Q_{ok}}\dfrac{2M_{gk}}{D}\\ T_{ok}=\dfrac{Q_{ok}}{Q_{ik}+Q_{ok}}\dfrac{2M_{gk}}{D}\end{cases} \tag{13}$$

thus

$$\begin{cases}\lambda_{ik}=\dfrac{Q_{ik}}{Q_{ik}+Q_{ok}}\\ \lambda_{ok}=\dfrac{Q_{ok}}{Q_{ik}+Q_{ok}}\end{cases} \tag{14}$$

Based on the above analysis, the vector equilibrium equation of ball can be further simplified as:

$$\overrightarrow{F_{ck}}+\overrightarrow{F_{ik}}+\overrightarrow{F_{ok}}=0 \tag{15}$$

$$\begin{cases}\overrightarrow{F_{ik}}=\overrightarrow{Q_{ik}}+\overrightarrow{T_{ik}}\\ \overrightarrow{F_{ok}}=\overrightarrow{Q_{ok}}+\overrightarrow{T_{ok}}\end{cases} \tag{16}$$

As shown in Fig. 2(b), according to the sine theorem of plane triangle:

$$\frac{F_{ik}}{\sin\theta_{ok}} = \frac{F_{ok}}{\sin\theta_{ik}} = \frac{F_{ck}}{\sin(\theta_{ik}-\theta_{ok})} \tag{17}$$

$$\begin{cases}\theta_{ik} = \alpha_{ik} - \Delta\alpha_{ik} \\ \theta_{ok} = \alpha_{ok} - \Delta\alpha_{ok}\end{cases} \tag{18}$$

According to Eqs. (12) and (13), one can obtain:

$$\Delta\alpha = \Delta\alpha_{ik} = \Delta\alpha_{ok} = \arctan\left(\frac{1}{Q_{ik}+Q_{ok}}\frac{2M_{gk}}{D}\right) \tag{19}$$

$$\theta_{ik} - \theta_{ok} = \alpha_{ik} - \alpha_{ok} \tag{20}$$

therefore

$$\begin{cases}F_{ik} = \dfrac{\sin(\alpha_{ok}-\Delta\alpha)}{\sin(\alpha_{ik}-\alpha_{ok})}F_{ck} \\ F_{ok} = \dfrac{\sin(\alpha_{ik}-\Delta\alpha)}{\sin(\alpha_{ik}-\alpha_{ok})}F_{ck}\end{cases} \tag{21}$$

In addition, the ball-raceway contact loads Q_{ik} and Q_{ok} can be written as:

$$\begin{cases}Q_{ik} = F_{ik}\cos\Delta\alpha \\ Q_{ok} = F_{ok}\cos\Delta\alpha\end{cases} \tag{22}$$

Besides, the centrifugal force and gyroscopic moment of ball can be expressed:

$$\begin{cases}F_{ck} = 0.5md_m\omega_{mk}^2 \\ M_{gk} = J\omega_{mk}\omega_{bk}\sin\beta_k\end{cases} \tag{23}$$

where the angular speeds ω_{mk} and ω_{bk} denote the revolution speed and spinning speed of ball, respectively. m and J denote the mass and mass moment of ball. And the angular speeds ω_{mk} and ω_{bk} can be obtained according to the assumption that no macroscopic sliding phenomenon occurs in ball-raceway contact zones:

$$\begin{cases}\omega_{mk} = \dfrac{\omega_i(1-\gamma_{ik})\cos(\alpha_{ok}-\beta_k)}{(1+\gamma_{ok})\cos(\alpha_{ik}-\beta_k)+(1-\gamma_{ik})\cos(\alpha_{ok}-\beta_k)} \\ \omega_{bk} = \dfrac{d_m}{D}\dfrac{\omega_i(1-\gamma_{ik})(1+\gamma_{ok})}{(1+\gamma_{ok})\cos(\alpha_{ik}-\beta_k)+(1-\gamma_{ik})\cos(\alpha_{ok}-\beta_k)}\end{cases} \tag{24}$$

$$\begin{cases}\gamma_{ik} = D\cos\alpha_{ik}/d_m \\ \gamma_{ok} = D\cos\alpha_{ok}/d_m\end{cases} \tag{25}$$

Usually, the ball pitch angle β_k is also calculated by the raceway control hypothesis that the ball has no spinning motion on the "control raceway". However, it has been proved that the spinning speed between ball and outer raceway tends toward zero only when ball bearing is operated at high-speed and light load conditions. In order to overcome the limitations of the raceway control hypothesis, the d'Alembert principle without raceway control hypothesis is used for ball pitch angle calculation [7]:

$$\tan\beta_k = \frac{C(S+1)\sin\alpha_{ik} + 2\sin\alpha_{ok}}{C(S+1)\cos\alpha_{ik} + 2(\cos\alpha_{ok} + D/d_m) + G} \tag{26}$$

$$\begin{cases}C = \dfrac{Q_{ik}a_{ik}L_{ik}}{Q_{ok}a_{ok}L_{ok}} \\ G = \dfrac{D}{d_m}C\left[\cos(\alpha_{ik}-\alpha_{ok}) - S\right] \\ S = \dfrac{1+D/d_m\cos\alpha_{ok}}{1-\cos\alpha_{ik}}\end{cases} \tag{27}$$

where a_{ik} and a_{ok} the semi-major axis of ball-inner raceway and ball-outer raceway contacts, respectively, and L_{ik} and L_{ok} are the second kind elliptic integral of ball-inner raceway and ball-outer raceway contacts, respectively.

Through the above analysis of local ball, it can be found that only two unknown variables α_{ik} and α_{ok} have appeared in the ball modeling, and other intermediate variables can be explicitly expressed by the variables α_{ik} and α_{ok}. Therefore, for a given global displacement vector **d** = {δ_x, δ_y, δ_z, θ_y, θ_z}, the unknown variables α_{ik} and α_{ok} can be obtained by solving the implicit Eq. (3) based on the Newton-Raphson method. Compared to the classical Jones' model of ball bearing, the improved model has three obvious advantages: (1) The number of unknown variables for single ball reduces from four to two, thus greatly reduces the computation load in the single iterative calculation; (2) using the ball-raceway contact angles with clear physical meaning as the iterative variables can facilitate the selection of the iterative initial values; (3) due to the abandonment of raceway control hypothesis, the applicability and accuracy of the model are improved.

On the basis of local ball analysis, the global equilibrium equations of inner ring can be written as:

$$\begin{cases}F_x = \sum_1^Z F_{ik}\sin\theta_{ik} \\ F_y = \sum_1^Z F_{ik}\cos\theta_{ik}\cos\psi_k \\ F_z = \sum_1^Z F_{ik}\cos\theta_{ik}\sin\psi_k \\ M_y = \dfrac{d_m}{2}\sum_1^Z F_{ik}\sin\theta_{ik}\sin\psi_k \\ M_z = -\dfrac{d_m}{2}\sum_1^Z F_{ik}\sin\theta_{ik}\cos\psi_k\end{cases} \tag{28}$$

In order to solve the above global equilibrium equations of ring and local equilibrium equations of balls, a nested-loop iteration algorithm is given in Fig. 3. Firstly, input the basic

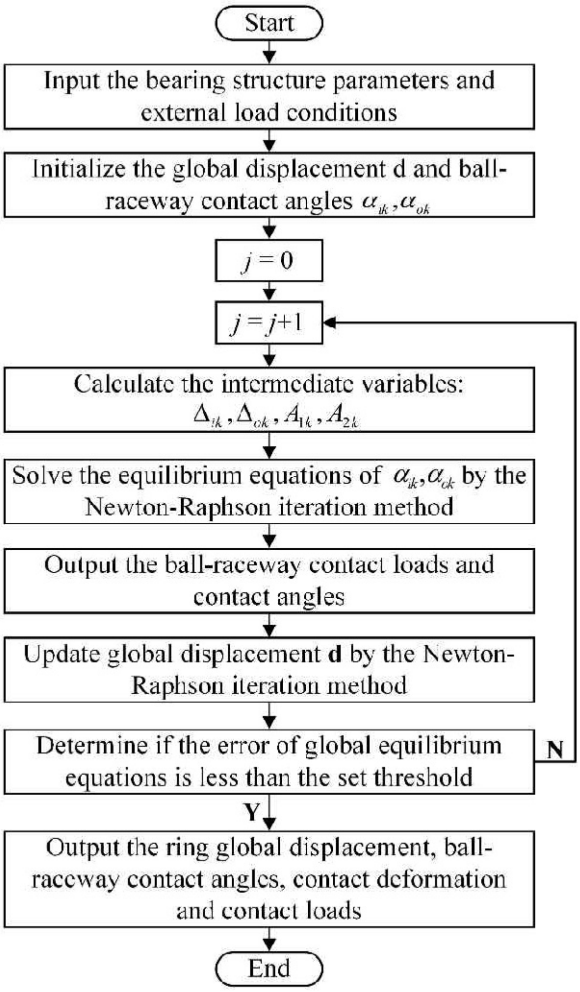

Fig. 3. The detailed calculation flow of the proposed model.

structural parameters and operation condition of ball bearing and give the proper iterative initial values of the global displacement vector **d** = { δ_x , δ_y , δ_z , θ_y , θ_z } and ball-raceway contact angles α_{ik} and α_{ok} ; secondly, solve the local equilibrium equations of ball and update the values of ball-raceway contact angles α_{ik} and α_{ok} ; then, substitute the new local variables into the global equilibrium equations of ring and update the values of the global displacement vector **d** = { δ_x , δ_y , δ_z , θ_y , θ_z }; repeat the above iteration until the calculation error is less than the set threshold; finally, output the final values of global displacement vector **d** and ball-raceway contact angles α_{ik} and α_{ok} .

3. Results and discussion

Based on the model proposed above, the angular contact ball bearing B218 under different operation conditions was studied and analyzed, and the detailed structural parameters of B218 are listed in Table 1. To validate the correctness of the proposed model, the comparison results of ball-raceway contact angles calculated by the proposed model and Jones' model with two different raceway control hypotheses are given in Figs. 4-8.

Table 1. The structural parameters of B218.

Parameters	B218
Bearing inner raceway curvature radius r_i (mm)	11.6281
Bearing outer raceway curvature radius r_o (mm)	11.6281
Bearing inner raceway contact diameter d_i (mm)	102.7938
Bearing outer raceway contact diameter d_o (mm)	147.7264
Number of balls Z	16
Ball diameter D (mm)	22.225
Pitch diameter d_m (mm)	125.26

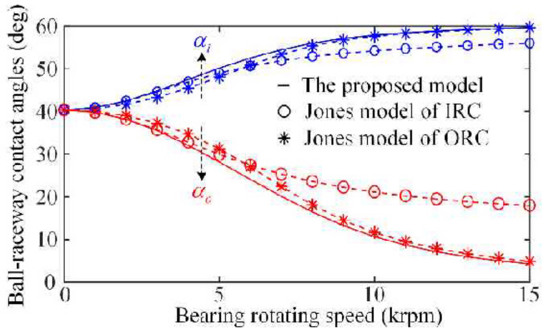

Fig. 4. The comparison curves of speed-varying contact angles between the proposed model and the Jones' model.

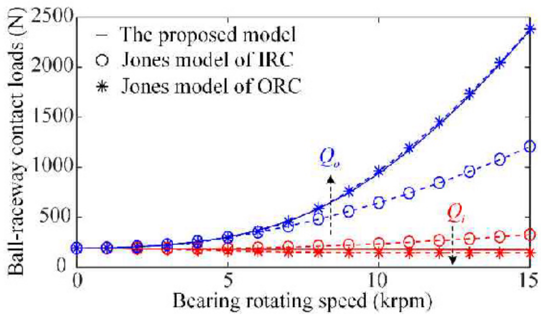

Fig. 5. The comparison curves of speed-varying contact loads between the proposed model and the Jones' model.

As shown in Fig. 4, the results of the speed-varying contact angles of ball bearing under a constant axial load (F_x = 2000 N) obtained by the proposed model and Jones' model with the Inner and outer raceway control hypotheses (I/ORC Hypothesis) are presented. It can be found that, the change curves of ball-raceway contact angles obtained by three different methods have a similar law. By further comparing the three result curves, it also can be found that, the result curve by the proposed model is relatively close to that obtained by Jones' model with IRC hypothesis at low speed range and relatively close to that of Jones' model with ORC hypothesis at high speed range. Meanwhile, the similar law can also been found in the results of speed-varying ball-raceway contact loads and ball pitch angle as shown in Figs. 5 and 6. By reviewing the

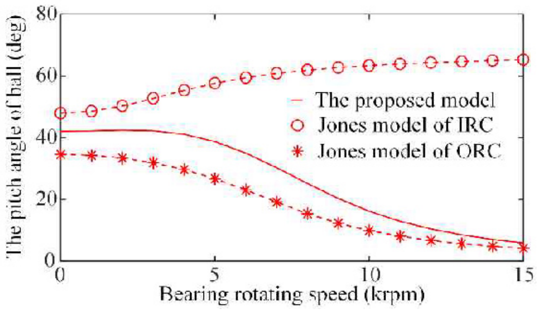

Fig. 6. The comparison curves of speed-varying pitch angle between the proposed model and the Jones' model.

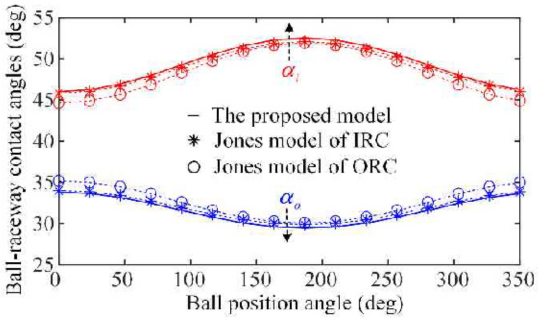

Fig. 7. The comparison results of the ball-raceway contact angles under the given displacement vector **d** = {10 um, 15 um, 0, 0, 0}.

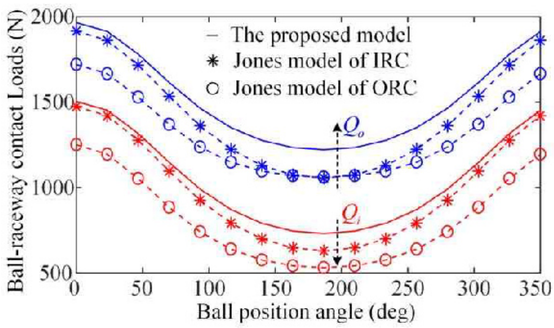

Fig. 8. The comparison results of the ball-raceway contact loads under the given displacement vector **d** = {10 um, 15 um, 0, 0, 0}.

application conditions and scopes of two different raceway control hypotheses: The IRC Hypothesis is more applicable for ball bearing at low speed range and ORC hypothesis is more applicable for ball bearing at high speed range. It is indicated that the proposed model without raceway control hypothesis has a higher applicability and rationality compared to Jones' model with different raceway control hypotheses.

In order to further validate the correctness of the proposed model, the results of ball-raceway contact angles and loads of ball bearing under the given displacement vector **d** = {10 um, 15 um, 0, 0, 0} are shown in Figs. 7 and 8. It can be found that the results of the proposed model show a good agreement with those of Jones' model with two different raceway control hypotheses.

Based on the proposed model, the results of the ball-

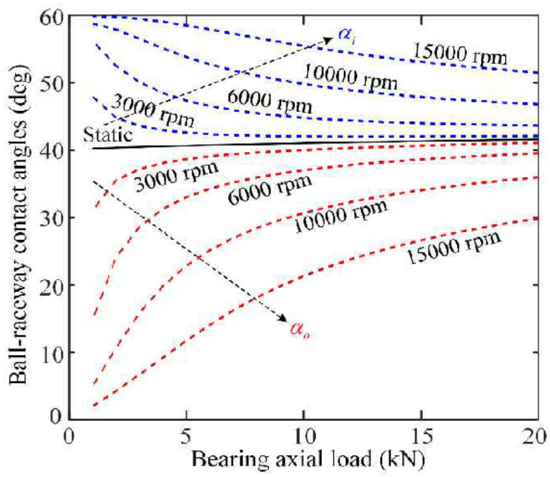

Fig. 9. The results of the ball-raceway contact angles against the axial loads of ball bearing under different speeds.

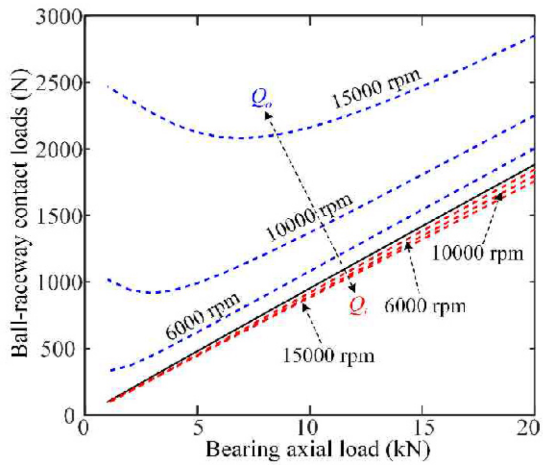

Fig. 10. The results of the ball-raceway contact loads against the axial loads of ball bearing under different speeds.

raceway contact angles and loads varying with the axial loads for ball bearing under different speeds are given in Figs. 9 and 10. As shown in Fig. 9, for ball bearing under the constant axial load, with the increase of rotating speed, the ball-inner raceway contact angle α_i increases and ball-outer raceway contact angle α_o decreases. In addition, for ball bearing under the constant rotating speed, with the increase of axial load, the ball-inner raceway contact angle α_i decreases and ball-outer raceway contact angle α_o increases. It means that axial load can effectively reduce the difference between contact angles α_i and α_o caused by the ball inertia forces.

Besides, it can be seen from Fig. 10, for ball bearing under the constant axial load, with the increase of rotating speed, the ball-outer raceway contact load Q_o increases and ball-inner raceway contact load Q_i basically remains unchanged. In addition, for ball bearing at the high speed range, with the increase of axial load, the ball-outer raceway contact load Q_o first decreases and then increases and ball-outer raceway contact load Q_i increases linearly.

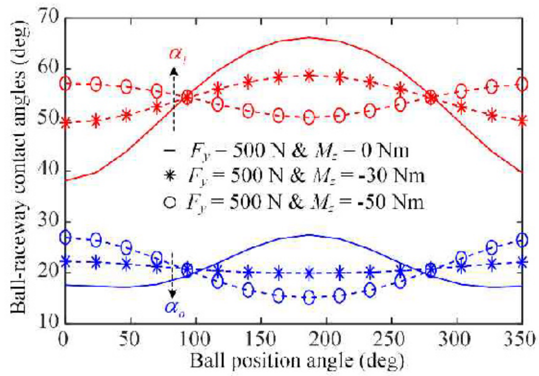

Fig. 11. The contact angles distribution of ball bearing under different combined loads conditions.

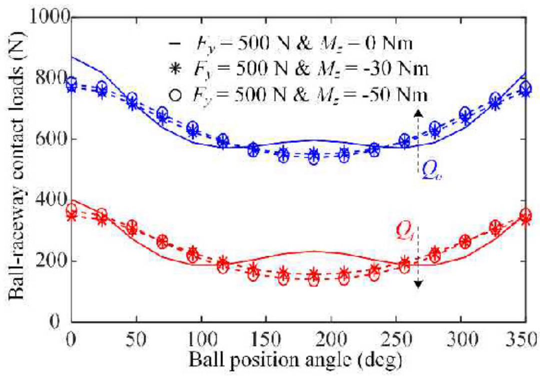

Fig. 12. The contact loads distribution of ball bearing under different combined loads conditions.

Different from the above analysis of ball bearing under the pure axial load, the studies of ball bearing under different combined load conditions and 10000 rpm have been conducted and the relevant results have been presented in Figs. 11 and 12. Without loss of generality, it is assumed that ball bearing is subjected to the constant axial load (F_x = 2000 N) and radial load (F_y = 500 N), then the coupling mechanism of radial and moment loads is studied by changing the size of moment load M_z. It can be seen from Figs. 11 and 12, when the moment load is equal to zero, the ball-raceway contact angles and loads at different angular positions present a distinct uneven distribution that is harmful for the fatigue life and dynamic performance of ball bearing. As a certain amount of reverse moment load (M_z = -30 Nm) applied, the ball-raceway contact angles and loads at different angular positions tend to be equal, it indicates that the uneven load distribution caused by the radial load can be improved by the moment load with a certain direction and size. However, as the moment load further increases (M_z = -50 Nm), the distribution states of ball-raceway contact angles and loads are deteriorated again. Above all, for ball bearing subjected to the radial load, a proper moment load with the certain direction and size can be used to improve the load distribution and service performance of ball bearing. Meanwhile, the above analysis also gives a good explanation of the action mechanism for the non-uniform preload mechanism and provides a theoretical guidance for the selection of the size and distribution scheme of non-uniform preload [17-19].

4. Conclusions

Based on the various contact angles and the hybrid theory without the raceway control hypothesis, this paper presents a new efficient and accurate algorithm for the performance prediction of ball bearing under the combined axial, radial and moment loads. In the proposed model, the triangular geometric theorem and vector diagram method are used in the force analysis of local ball instead of the orthogonal decomposition method, thus effectively reducing the computation load of bearing model. Then, the contact angles and loads of ball bearing under different operation conditions are calculated, and partial results are compared with the Jones' model with two different raceway control hypotheses (IRC/ORC) to verify the correctness of the present model. Besides, the results show that the axial load can effectively reduce the difference between ball-raceway contact angles α_i and α_o, and a proper moment load can be used to improve the load distribution and service performance of ball bearing under the action radial load.

Acknowledgments

This work is supported by the National Natural Science Foundation of China (51635010) and Henan Key Laboratory of High-performance Bearings, Luo Yang 471003, China (2016 ZCKF01).

References

[1] R. Stribeck, Ball bearing for various loads, *Transactions of the ASME*, 29 (1907) 420-463.
[2] H. Sjovall, The load distribution within ball and roller bearings under given external radial and axial load, *Teknisk Tidskrift*, 19 (3) (1933) 72-75.
[3] G. Lundberg, Dynamic capacity of roller bearings, *Mechanical Engineering*, 4 (2) (1952) 96-127.
[4] A. Palmgren, *Ball and Roller Bearing Engineering*, Philadelphia: SKF Industries Inc. (1959).
[5] A. B. Jones, A general theory for elastically constrained ball and radial roller bearings under arbitrary load and speed conditions, *Journal of Basic Engineering*, 82 (2) (1960) 309-320.
[6] T. A. Harris, *Rolling Bearing Analysis*, 4th Edition, John Wiley and Sons, Inc., New York (2000).
[7] C. A. Ding et al., Raceway control assumption and the determination of rolling element attitude angle, *Chinese Journal of Mechanical Engineering*, 37 (2) (2001) 58-61.
[8] W. Z. Wang et al., Modeling angular contact ball bearing without raceway control hypothesis, *Mechanism and Machine Theory*, 82 (2014) 154-172.
[9] C. A. Foord, High-speed ball bearing analysis, *Proceedings of the Institution of Mechanical Engineers Part G: Journal of*

Aerospace Engineering, 220 (5) (2006) 537-544.
[10] T. A. Harris, An analytical method to predict skidding in thrust-loaded, angular-contact ball bearings, *Journal of Lubrication Technology*, 93 (1) (1971) 17-24.
[11] N. T. Liao and J. F. Lin, A new method for the analysis of deformation and load in a ball bearing with variable contact angle, *Journal of Mechanical Design*, 123 (2) (2001) 304-312.
[12] N. T. Liao and J. F. Lin, A new method developed for the analysis of ball bearing fatigue life considering variable contact angles, *Tribology Transactions*, 46 (3) (2003) 435-446.
[13] N. T. Liao and J. F. Lin, An analysis of misaligned single-row angular-contact ball bearing, *Journal of Mechanical Design*, 126 (2) (2004) 370-374.
[14] Y. Guo and R. G. Parker, Stiffness matrix calculation of rolling element bearings using a finite element/contact mechanics model, *Mechanism and Machine Theory*, 51 (2012) 32-45.
[15] J. F. Antoine, G. Abba and A. Molinari, A new proposal for explicit angle calculation in angular contact ball bearing, *Journal of Mechanical Design*, 128 (2) (2006) 468-478.
[16] B. Fang, J. H. Zhang, J. Hong and Y. S. Zhu, Quick calculation method and contact angle analysis for high-speed angular contact ball bearing under combined loads, *Hsi-An Chiao Tung Ta Hsueh/Journal of Xi'an Jiaotong University*, 51 (6) (2017) 115-121.
[17] X. Li, H. Li, Y. Z and J. Hong, Investigation of non-uniform preload on the static and rotational performances for spindle bearing system, *International Journal of Machine Tools and Manufacture*, 106 (2016) 11-21.
[18] X. H. Li et al., Experiment analysis of spindle performance with rolling bearing under non-uniform preload, *ARCHIVE Proceedings of the Institution of Mechanical Engineers Part C: Journal of Mechanical Engineering Science*, 230 (17) (2015) 203-210.
[19] Y. Zhang et al., Uneven heat generation and thermal performance of spindle bearings, *Tribology International*, 126 (2018).

Jin-hua Zhang received his Ph.D. from Xi'an Jiaotong University at the Department of Mechanical Engineering in 2008. He is now an Associate Professor at the Key Laboratory of Education Ministry for Modern Design and Rotor-Bearing System and State Key Laboratory for Manufacturing Systems Engineering. His specialty includes rolling bearing and rotor dynamics, soft robotics, Multibody and nonlinear dynamics, tribology, mechanical design and multi-objective optimization, brain-machine interface.